New Phytologist

Research

Different levels of energetic coupling between photosynthesis and respiration do not determine the occurrence of adaptive responses of Symbiodiniaceae to global warming

Mattia Pierangelini[1], Marc Thiry[2] and Pierre Cardol[1]

[1]Génétique et Physiologie des Microalgues, InBioS/Phytosystems, Institut de Botanique, Université de Liège, B22, Liège 4000, Belgium; [2]Unit of Cell Biology, GIGA-Neurosciences, CHU Sart-Tilman, University of Liège, Liège B36, 4000, Belgium

Authors for correspondence:
Mattia Pierangelini
Tel: +32 (0)43 66 38 40
Email: mattia.pierangelini@gmail.com

Pierre Cardol
Tel: +32 (0)43 66 38 40
Email: Pierre.Cardol@uliege.be

Received: *14 March 2020*
Accepted: *30 May 2020*

New Phytologist (2020) **228:** 855–868
doi: 10.1111/nph.16738

Key words: adaptation, alternative oxidase, CO_2 acquisition, climate change, coral reefs, metabolism, symbiosis, temperature.

Summary

- Disentangling the metabolic functioning of corals' endosymbionts (Symbiodiniaceae) is relevant to understanding the response of coral reefs to warming oceans. In this work, we first question whether there is an energetic coupling between photosynthesis and respiration in Symbiodiniaceae (*Symbiodinium*, *Durusdinium* and *Effrenium*), and second, how different levels of energetic coupling will affect their adaptive responses to global warming.
- Coupling between photosynthesis and respiration was established by determining the variation of metabolic rates during thermal response curves, and how inhibition of respiration affects photosynthesis. Adaptive (irreversible) responses were studied by exposing two *Symbiodinium* species with different levels of photosynthesis–respiration interaction to high temperature conditions (32°C) for 1 yr.
- We found that some Symbiodiniaceae have a high level of energetic coupling; that is, photosynthesis and respiration have the same temperature dependency, and photosynthesis is negatively affected when respiration is inhibited. Conversely, photosynthesis and respiration are not coupled in other species. In any case, prolonged exposure to high temperature caused adjustments in both photosynthesis and respiration, but these changes were fully reversible.
- We conclude that energetic coupling between photosynthesis and respiration exhibits wide variation amongst Symbiodiniaceae and does not determine the occurrence of adaptive responses in Symbiodiniaceae to temperature increase.

Introduction

The Symbiodiniaceae family (dinoflagellates, LaJeunesse *et al.*, 2018) comprises microalgae species capable of establishing endosymbiotic relationships with animal hosts such as Cnidaria, Porifera and Mollusca (Leggat *et al.*, 1999; Weber & Medina, 2012; Achlatis *et al.*, 2018). This association between Symbiodiniaceae and their hosts is key to the integrity and functioning of coral reef ecosystems world-wide. Under current climate change conditions, alterations of global temperatures have been identified as major threats to coral reefs (Spalding & Brown, 2015; Hughes *et al.*, 2017a,b). Increasing mean water temperatures, together with extreme climatic events such as heat waves, are disrupting the endosymbiotic relationship between Symbiodiniaceae and their cnidarian hosts, and causing reef death if these events are persistent and severe (Suggett *et al.*, 2017; Hughes *et al.*, 2018; Fordyce *et al.*, 2019; Goyen *et al.*, 2019).

In the future, the response of coral reefs to changes in temperature will depend on the ability of both Symbiodiniaceae and their hosts to adapt to the new climatic conditions (Chakravarti *et al.*, 2017; Torda *et al.*, 2017; Comeau *et al.*, 2019). Because of their large population size, short generation times (at least under a free-living lifestyle) and high genetic diversity, Symbiodiniaceae species are expected to have a faster adaptive capacity to climatic changes than their hosts (Collins, 2011; Torda *et al.*, 2017; Comeau *et al.*, 2019; González-Pech *et al.*, 2019). Thus, studies of isolated Symbiodiniaceae provide valuable contributions to the understanding of the mechanisms underpinning corals' adaptation to ocean warming. Recent studies focusing on the responses of these organisms to long-term temperature increases have shown that some isolated Symbiodiniaceae are capable of relatively fast adaptation (*c.* 2.5 yr and 80 cell generations) to elevated temperature conditions (Huertas *et al.*, 2011; Chakravarti *et al.*, 2017; Chakravarti & van Oppen, 2018).

Adaptation (long-term irreversible responses, usually requiring *de novo* mutations in the genome or species sorting) to warming conditions could imply modifications of the two most important metabolic processes of the algal cell, photosynthesis and respiration. In photosynthetic organisms (both plants and algae), photosynthesis and respiration occur in different organelles (chloroplasts and mitochondria, respectively), and their activities are very often coupled (Raghavendra & Padmasree, 2003; Cardol

et al., 2009). In the green alga *Chlamydomonas reinhardtii*, mitochondrial respiration can supply ATP to the chloroplast, influencing net CO_2 fixation (Cardol *et al.*, 2009) and affecting the photosynthetic response under high light intensity conditions (Larosa *et al.*, 2018). Similarly, energetic interaction (exchanging ATP and NADPH) between the mitochondrion and the chloroplast occurs in diatoms (Bailleul *et al.*, 2015). In regard to Symbiodiniaceae and other dinoflagellates, it is still unknown whether respiration activity is energetically connected to photosynthesis. The possible presence of phenotypes with multiple degrees of photosynthesis to respiration coupling is also unexplored. Disentangling the extent of photosynthesis dependence on respiration is fundamental to clarifying the adaptive capability of photosynthesis and respiration of Symbiodiniaceae under future climatic conditions.

In relation to other species, thermal response curve (TRC) analyses (i.e. by measuring photosynthetic and respiratory responses to acute increases in temperature), showed that green algae adaptation (over several hundred cell generations) to high (above-optimal) temperature conditions involves either increasing the rates of photosynthesis or lowering the rates of respiration (Padfield *et al.*, 2016; Schaum *et al.*, 2017). By contrast, in the marine diatom *Thalassiosira pseudonana*, adaptation to different warming scenarios caused a similar decline in both photosynthetic and respiration rates (Schaum *et al.*, 2018). However, these studies did not establish whether the effects were due to adaptation or acclimation (i.e. short-term reversible responses) (Raven *et al.*, 2017). Particularly for respiration, exposure to elevated temperatures may also cause two types of response in the respiration TRCs: type I (involving changes of the slope of the TRCs) and type II (reduction in the elevation of the TRC) (Atkin & Tjoelker, 2003; Smith & Dukes, 2013). In this work, using Symbiodiniaceae as model species, we question the extent to which the degree of coupling between photosynthesis and respiration influences adaptive responses (measured through TRCs) to warming conditions (Atkin *et al.*, 2006).

Photosynthetic adaptation to increasing temperature will also possibly require adjustments in mechanisms of inorganic carbon (C_i) acquisition. To acquire C_i, Symbiodiniaceae possess a CO_2-concentrating mechanism (CCM), that is, structural and functional components which enhance intracellular levels of C_i and favour the carboxylation activity of their form II Rubisco (Leggat *et al.*, 1999; Brading *et al.*, 2011, 2013; Ros *et al.*, 2020). Generally, CCM activity is modulated by the changing of thermal conditions (Beardall & Giordano, 2002; Giordano *et al.*, 2005), and CCM functioning could be linked to species adaptation to cold (or warm) habitats (Kranz *et al.*, 2015; Raven *et al.*, 2017). In the case of Symbiodiniaceae, Oakley *et al.* (2014a) showed that acclimation to high thermal regimes over several wk resulted in a higher photosynthetic affinity for C_i (reflecting enhanced CCM activity), which could be induced by the lower CO_2 solubility in water or a lower Rubisco CO_2 : O_2 selectivity factor (Tcherkez *et al.*, 2006; Raven *et al.*, 2017). However, no information is currently available on the adaptive capability of CCMs in Symbiodiniaceae under long-term changes in temperature conditions.

In this work, we first aimed to establish whether there is an energetic coupling between photosynthesis and respiration, and the extent to which this interplay occurs in Symbiodiniaceae (from three genera, namely *Symbiodinium*, *Durusdinium* and *Effrenium*). Second, we explored the consequences of two different levels of coupling between photosynthesis and respiration for the adaptive capabilities of Symbiodiniaceae to a 1-yr increase in temperature. Finally, we assessed the extent to which adaptation of photosynthesis to warmer conditions is associated with phenotypical adjustments of CCM activity.

Materials and Methods

Organisms and culture conditions

Four species belonging to three different genera of the Symbiodiniaceae family (*Symbiodinium* Freudenthal, *Durusdinium* LaJeunesse and *Effrenium* LaJeunesse et Jeong) were studied. These included *Symbiodinium* sp. (Avir), *Symbiodinium* sp. (Stylodid), *Durusdinium trenchii* (provided by Annika Guse, University of Heidelberg), and *Effrenium voratum* (Table 1). To confirm the classification of these species at the genus and/or species level, the sequencing of 5.8S rDNA internal transcribed space 2 (ITS2) regions was carried out as described in Hume *et al.* (2018). For all the experiments, cells were cultured in F/2 medium, prepared with sea salt (Coral Pro Salt, Red Sea; Red Sea Fish Pharm, Verneuil d'Avre et d'Iton, France) and Guillard's (F/2) Marine Water Enrichment Solution (Sigma-Aldrich), with a total dissolved inorganic carbon (C_i) content of 4 mM (CO_2 = 20 μM; HCO_3^- = 3495 μM; calculated using the CO2Sys.xls application, Lewis & Wallace, 1998), Alk = 4.5 mEq l^{-1}, a salinity of 34 PSU, and buffered at pH 8.1 using 20 mM Tris-HCl. Cultures of *Symbiodinium* sp. (Avir and Stylodid) and *E. voratum* were maintained in a plant growth chamber (Grobanks; CLF Plant Climatics GmbH, Wertingen, Germany) and exposed to a continuous photosynthetic photon flux density (PPFD) of 100 μmol photons m^{-2} s^{-1}. Because this light regime was not suitable for the growth of *D. trenchii*, this species was maintained with a PPFD of *c*. 20 μmol photons m^{-2} s^{-1} under a 12 h : 12 h, light : dark photoperiod. Experiments were conducted for *D. trenchii* at least 3 h after the onset of the light period. For the control temperature condition, cultures of *Symbiodinium* sp. (Avir and Stylodid), *E. voratum* and *D. trenchii* were maintained at 25°C. During the experiments, cell concentration in the culture was maintained below 150 000–200 000 cells ml^{-1} by regular sub-culturing with fresh F/2 medium. Although cultures were not axenic, bacterial concentration was always low (as verified by regular microscope inspection).

Cell concentration was determined using a Coulter counter (Z2; Beckman, Indianapolis, IN, USA). The cell-specific division rates (μ_c) of *Symbiodinium* sp. (Avir), *Symbiodinium* sp. (Stylodid), and *E. voratum* were calculated from the slope of the natural logarithm plot, obtained from the exponential phase of the population growth in the culture. As *D. trenchii* was maintained under a lower light regime and a light : dark cycle, conditions

Table 1 Symbiodiniaceae species used in this study.

Culture name	Species (Former clade)	Host species (Type of host)	Geographic origin (Temperature min–max)	Collection
Avir	*Symbiodinium* sp. (A)	*Anemonia viridis* (Sea anemone)	Mediterranean Sea, France (13–25°C)	Paola Furla, University of Nice
Stylodid	*Symbiodinium* sp. (A)	*Stylophora pistillata* (Coral)	Red Sea (21–28°C)	Centre Scientifique De Monaco collection
CCMP2556	*Durusdinium trenchii* (D)	*Montastraea faveolata* (Coral)	Tennessee Reef, Florida Keys, Florida, USA (22–28°C)	Mary Alice Coffroth
CCMP421	*Effrenium voratum* (E)	Free-living	Wellington, New Zealand (22–26°C)	Mary Alice Coffroth

which would affect the comparison with cells exposed to continuous light (Quigg *et al.*, 2012), its μ_c value was not estimated.

Long-term exposure to elevated temperature

For the long-term exposure to elevated temperature, three independent replicate cultures of *Symbiodinium* sp. (Avir and Stylodid) were transferred at 32°C and kept under this regime for 1 yr. These two species have been previously assessed for short-term acclimation responses at 33°C (Dang *et al.*, 2019), and as they belong to the same genus and both have a facultative symbiotic lifestyle, they provide a solid basis for the present comparison. We chose 32°C because it reflects the warming conditions that tropical algal species might experience in future years due to climate change (IPCC, 2014; Jin & Agustí, 2018; Aranguren-Gassis *et al.*, 2019). During the 1 yr of incubation at 32°C, cultures were diluted with new F/2 medium (pH 8.1; CO_2 = 17 μM; HCO_3^- = 3368 μM) every 7 d in the case of *Symbiodinium* sp. (Avir) and every 14 d for *Symbiodinium* sp. (Stylodid), according to their different μ_c under the 32°C treatment (Fig. 5). The μ_c, photosynthesis and respiration activities were analysed after 5, 7 and 12 months from the start of the 32°C incubation period. According to their μ_c values, the 1-yr-long experiment equated to *c.* 310 and 190 cell generations for *Symbiodinium* sp. (Avir) and *Symbiodinium* sp. (Stylodid) respectively. To test whether the physiological traits displayed during such long-term exposure were stable and adaptive, at the end of the 1-yr period of warming, cells were returned for at least 1 wk to the control temperature of 25°C (Chakravarti *et al.*, 2017). Only measurements showing adaptive photosynthetic and/or respiratory adjustments were repeated.

Measurements of photosynthetic and respiratory activities

Rates of photosynthetic O_2 evolution as a function of irradiance (P vs I curve) and dark respiration (R_d) were measured with a Clark-type oxygen electrode (Hansatech, Norfolk, UK). P vs I curves were measured for all species grown at 25°C and *Symbiodinium* sp. (Avir and Stylodid) at 32°C. For each experiment, cells were concentrated through centrifugation at 2200 ***g*** for 2 min. As Symbiodiniaceae cells are large (*c.* 10 μm, Roberty *et al.*, 2014), harvesting by low centrifugation force allows the sinking and formation of a pellet at the bottom of the centrifuge tube, and the separation of the smaller prokaryotic cells which remain in the supernatant (Malerba *et al.*, 2018). After centrifugation, the cells were resuspended in 1 ml of fresh culture F/2 medium (+2 mM $NaHCO_3$) and placed into the electrode chamber. Before each P vs I measurement, the cells were dark acclimated for 15 min, with the final 5 min of this incubation period used to measure the R_d. After the dark pre-treatment, O_2 evolution inside the chamber was measured over a range (4–1350 μmol photons m^{-2} s^{-1}) of PPFD, provided by an LED light source peaking at 630–640 nm. Gross photosynthesis (P) was calculated as the sum of R_d and net photosynthesis. During the experiments, to avoid the possibility of photorespiration (Oakley *et al.*, 2014a; Ros *et al.*, 2020) and a potential underestimation of O_2 evolution rates due to O_2 saturation, the O_2 concentration in the chamber was maintained below *c.* 80% of air equilibrium.

Thermal response curves

We carried out TRCs as in Karsten & Holzinger (2012) and Pierangelini *et al.* (2019). For these analyses, cells were harvested from the culture by centrifugation (2200 ***g***, 2 min), resuspended in 1 ml of fresh culture F/2 medium (+2 mM $NaHCO_3$), and placed into a Clark-type oxygen electrode chamber (Hansatech Norfolk, UK). TRCs were measured for all species grown at 25°C and *Symbiodinium* sp. (Avir and Stylodid) at 32°C. For TRCs, cells were exposed to rising temperatures from 15 to 40°C. In the case of *Symbiodinium* sp. (Avir) growing under control condition of 25°C, the starting temperature for TRCs was set at 10°C. The use of this lower initial temperature did not cause changes in the shape of the TRCs (Supporting Information Fig. S1a,b). However, when growing at 32°C, photosynthesis of *Symbiodinium* sp. (Avir) became more susceptible to low temperature (Fig. S1c), and TRCs were started at 15°C. At each temperature, cells were initially incubated in the dark for 25 min, with the last 10 min of this incubation period used to measure respiration. After the dark period, cells were exposed to a saturating PPFD of 700 μmol photons m^{-2} s^{-1} (LED light source peaking at 630–640 nm) for 10 min, with the final 5 min used to calculate the photosynthetic O_2 evolution. For each assay temperature, the oxygen electrode was calibrated (with air and N_2) and the oxygen electrode drift (O_2 depletion related to non-biological processes) was estimated in order to correct the raw O_2 evolution

and consumption data. Gross P was calculated as the sum of R_d and net photosynthesis. The activation energies (how quickly the trait varies as a function of temperature; Padfield *et al.*, 2016) of gross P (E_a P) and respiration (E_a R) were calculated from the slopes of the TRCs, using the Arrhenius equation $\log_e k = -E_a/R\,(1/T) + \log_e A$.

Impact of a respiratory inhibitor on photosynthesis

The effects of a respiratory inhibitor on photosynthesis were measured for all species grown at 25°C and *Symbiodinium* sp. (Avir and Stylodid) at 32°C. For these experiments, O_2 evolution and relative electron transport rate through the photosystem II (rETR) were recorded simultaneously with an optical O_2 meter – FireStingO_2 (Pyro Science, GmbH, Germany) and a JTS-10 spectrophotometer (Bio-logic, Claix, France) respectively, following the procedures of Roberty *et al.* (2014) and Vega de Luna *et al.* (2019). Prior to measurements, cells were incubated in the dark for 15 min. Salicylhydroxamic acid (SHAM) was diluted in DMSO (stock solution 1 M), and added at the beginning of the dark incubation period, with a final concentration in the cell suspension of 8 mM. This SHAM concentration is expected to cause a *c.* 20% reduction in respiration rates (Oakley *et al.*, 2014b). O_2 evolution and rETR were measured by exposing cells to a progressive increase (every *c.* 6 min) of PPFD (14–890 μmol photons m^{-2} s^{-1}) provided by an LED array emitting at 660 nm. During each light step intensity, F_s (stationary fluorescence level in light) and F'_m (maximum fluorescence emission induced by a saturating pulse > 5000 μmol photons m^{-2} s^{-1}) were measured, and the effective quantum yield of photosystem II at steady state (φPSII) was calculated as follows: $(F'_m - F_s)/F'_m$ (Genty *et al.*, 1989). The rETR was calculated as the product of φPSII and the actinic PPFD (Ralph & Gademann, 2005). Gross P was calculated as the sum of R_d and net photosynthesis.

Photosynthesis as a function of dissolved inorganic carbon

The photosynthesis of *Symbiodinium* sp. (Avir) under increasing inorganic carbon availabilities (P vs C_i) was measured using a Clark-type oxygen electrode (Leggat *et al.*, 1999; Treves *et al.*, 2016; Ruan *et al.*, 2017). For these measurements, we prepared F/2 culture medium depleted of C_i through acidification (pH ≤ 2) and bubbling with N_2 gas for at least 1 h. Shortly before the analysis, the F/2 C_i-free medium was re-adjusting to pH 8.1 with an NaOH pellet. For the experiment, cells were harvested from the culture, concentrated by centrifugation (2200 ***g***, 2 min), washed in 20 ml of F/2 C_i-free, resuspended in 990 μl of F/2 C_i-free, and placed in the electrode chamber, where they were exposed to a light saturating photosynthesis of 700 μmol photons m^{-2} s^{-1} (LED light source peaking at 630–640 nm). Photosynthesis was allowed to take place until the residual C_i in the F/2 medium and/or the intracellular C_i pool (Leggat *et al.*, 1999) were consumed, and a stable O_2 evolution rate was reached (after *c.* 2 h, minimizing potential photodamages related to C_i depletion). Photosynthetic rates were then measured over ascending $NaHCO_3$ concentrations (0–2000 μM), obtained by sequential additions (1–2 μl) of freshly prepared $NaHCO_3$ solutions (20, 100, 200 mM) into the O_2 electrode chamber. To estimate the photosynthetic affinity for CO_2, the slope of the CO_2-limited part of the P vs CO_2 curve, and the half saturation constant for CO_2-dependent photosynthesis ($K_{0.5}$ CO_2), were calculated (Pierangelini *et al.*, 2014; Ruan *et al.*, 2017). Slope of the C_i-limited part of the P vs C_i curves (not shown), and the half saturation constant for C_i-dependent photosynthesis ($K_{0.5}$ C_i) were also calculated.

Chl content

Chl cell contents were quantified as in Dang *et al.* (2019). Briefly, cells were harvested by centrifugation (2200 ***g***, 2 min), resuspended in 100% methanol and lysed in a TissueLyser II (30 Hz, 5 min, 4°C; Qiagen) in the presence of glass beads (710–1180 μm; Sigma-Aldrich). After debris removal at 4°C (by centrifugation at 10 000 ***g***, 10 min), Chl*a* and *c* concentrations were determined by spectrophotometry according to the equations of Ritchie (2006) for dinoflagellates.

Transmission electron microscopy

To evaluate whether the presence of different degrees of metabolic coupling between photosynthesis and respiration are associated with a different subcellular organization, analysis by transmission electron microscopy (TEM) was performed for *Symbiodinium* sp. (Avir) and *E. voratum*, the two most distant strains when considering interaction degree between respiration and photosynthesis. Cells samples for TEM were fixed in a vacuum bell for 2 h at 4°C with 2.5% glutaraldehyde in 0.1 M Sörensen's phosphate buffer (pH 7.4) and postfixed for 1.5 h with 2% osmium tetroxide. After washing in Sörensen's buffer, cells were dehydrated through graded ethanol solutions and then processed for embedding in Epon. Ultrathin sections of samples were contrasted with uranyl acetate and lead citrate before examination in a JEM 1400 transmission electron microscope at 80 kV (Jeol (Europe) BV, Zaventem, Belgium). Analysis of the TEM images and measurements of the sizes of the organelles were performed using the iTEM software (Olympus Soft Imaging Solutions GmbH, Münster, Germany). The number of mitochondria-chloroplast surface contacts were estimated in relation to the total number of chloroplastic sections contained in the cell, using at least 10 different randomly photographed cells. To estimate chloroplastic and mitochondrial sections sizes, at least 20 measurements were performed for each organelle.

Statistical analysis

Experiments were performed with at least three (unless otherwise stated) biological replicates per species. Comparisons between two treatments/species were made using two-tailed *t*-tests. When comparison involved more than two treatments/species, one-way ANOVA was used. Changes of parameters as a function of increasing temperature (TRCs) and changes during the yr-long experiment were tested using repeated measures (RM) ANOVA. All analyses were followed by Tukey's multiple comparisons test.

The analyses were performed using the software GraphPad Prism 5 (GraphPad Software, San Diego, CA, USA), setting the threshold of significance at 95%.

Results

TRCs show diverse degrees of metabolic thermal sensitivity amongst Symbiodiniaceae

To first establish whether gross O_2 evolution and dark respiratory O_2 consumption rates have either similar or different responses to an acute increase in temperature, we carried out TRCs. For the four Symbiodiniaceae (two *Symbiodinium* sp., *D. trenchii* and *E. voratum*), gross P increased from 10–15°C to 25–30°C, and declined beyond this range of temperatures (Fig. 1). The photosynthetic rates of *Symbiodinium* sp. (Avir and Stylodid) and *E. voratum* reached at 25°C were also comparable with the measures obtained with the P vs I curves (Table 2) (*t*-tests: $F_{3,2} = 17.38$, $P = 0.3554$; $F_{3,2} = 1.296$, $P = 0.0583$; $F_{2,2} = 1.694$, $P = 0.1420$, respectively), indicating that the rapid changes in temperature imposed during the TRCs did not impact the cell metabolisms. By contrast, the photosynthetic rates of *D. trenchii* were lower than those of the P vs I curves (Table 2) (*t*-tests: $F_{2,3} = 2.437$, $P = 0.0261$), reflecting a susceptibility of the species to the relatively low (15°C) initial temperature of the TRCs. In contrast to photosynthesis, respiration increased steadily during the heat exposure and did not decline at temperatures as high as 40°C. The comparison of the activation energy (E_a) parameter (in electron volts, eV), indicated that whereas the photosynthesis of the four species had different sensitivities to temperature (different E_a P) (ANOVA: $F_{2,7} = 91.01$, $P < 0.0001$), sensitivities of their respiratory activities to temperature were equivalent (similar E_a R; ANOVA: $F_{2,7} = 2.821$, $P = 0.1264$) (Fig. 2a). Comparing results in each species, differences were found in the temperature dependence of photosynthesis and respiration. The results showed that E_a P was higher than E_a R in both *Symbiodinium* sp. (Avir) (*t*-tests: $F_{3,3} = 10.14$, $P = 0.0004$) and *D. trenchii* (*t*-tests: $F_{2,2} = 4.120$, $P = 0.0021$). Conversely, in the case of *Symbiodinium* sp. (Stylodid) and *E. voratum*, E_a P was identical to E_a R (*t*-tests: $F_{2,2} = 57.36$, $P = 0.7885$; $F_{2,2} = 4.737$, $P = 0.1803$), indicating that both photosynthesis and respiration were equally sensitive to the temperature increase. These differences and similarities in temperature dependence were also indicated by the R_d : gross P ratios (Fig. 2b,c). Whereas for *Symbiodinium* sp. (Avir) and *D. trenchii*, the R_d : gross P ratio declined between the lowest and optimal temperatures (RM ANOVA: $F_{4,3,12} = 9.507$, $P = 0.0011$ and, $F_{2,2,4} = 14.72$, $P = 0.0143$), the R_d : gross P did not change (RM ANOVA: $F_{3,2,6} = 0.7479$, $P = 0.5620$ and, $F_{3,2,6} = 3.342$, $P = 0.0972$) for *Symbiodinium* sp. (Stylodid) and *E. voratum*.

Impacts of respiratory inhibitor reveal coupling between respiration and photosynthesis

The impact of inhibition (in the presence of SHAM) of the mitochondrial alternative oxidase (AOX) respiratory pathway on maximal photosynthetic capacity is reported in Fig. 3. Although chemical inhibitors might affect cell physiology at multiple levels (e.g. Roberty *et al.*, 2014), several studies have described SHAM as being capable of inhibiting the activity of the mitochondrial AOX pathway (but not other respiratory pathways) in several model algal species (Bailleul *et al.*, 2015; Larosa *et al.*, 2018; Murik *et al.*, 2019), including Symbiodiniaceae (Oakley *et al.*, 2014b). In our study, addition of 8 mM SHAM caused a mild 20–25% decrease in R_d in *Symbiodinium* sp. (Avir) (*t*-test: $F_{3,3} = 1.223$, $P = 0.0391$), *Symbiodinium* sp. (Stylodid) (*t*-test: $F_{2,2} = 1.570$, $P = 0.0001$), *D. trenchii* (*t*-test: $F_{2,2} = 1.746$, $P = 0.0177$), and *E. voratum* (*t*-test: $F_{5,5} = 1.103$, $P = 0.0328$). In relation to photosynthesis, addition of SHAM to *Symbiodinium* sp. (Avir), caused a *c.* 30% increase in the maximal rates of gross P (*t*-test: $F_{5,5} = 2.179$, $P < 0.0001$) but no changes in maximal rETR (*t*-test: $F_{5,5} = 2.465$, $P = 0.6271$) (Fig. 3). In the case of *Symbiodinium* sp. (Stylodid), the addition of SHAM caused a reduction in both maximal gross P (20%, *t*-test: $F_{5,5} = 1.702$, $P = 0.0339$) and maximal rETR (40%, *t*-test: $F_{5,5} = 1.306$, $P = 0.0047$). For *D. trenchii* and *E. voratum*, the addition of SHAM caused no alteration to their maximal gross P (*t*-test: $F_{5,5} = 1.582$, $P = 0.9962$; $F_{5,5} = 4.829$, $P = 0.1053$, respectively) but a *c.* 30% and 22%, respectively, decrease in the maximal rETR (*t*-test: $F_{5,5} = 1.651$, $P < 0.0001$; $F_{5,5} = 1.367$, $P = 0.0004$, respectively).

Subcellular organization does not reflect photosynthesis to respiration coupling

Transmission electron micrographs (Figs 4, S2) showed that both *Symbiodinium* sp. (Avir) and *E. voratum* contained an average of 10 chloroplastic sections (Lajeunesse *et al.*, 2010) per cell (*t*-test: $F_{13,13} = 3.736$, $P = 0.6960$). The number of mitochondrial sections in contact per chloroplastic section was *c.* 0.5 (± 0.1) for *Symbiodinium* sp. (Avir) and 0.6 (± 0.3) for *E. voratum*, with no differences between the two species (*t*-test: $F_{12,10} = 7.595$, $P = 0.6510$). The average values of chloroplastic section area per cell were 857 (± 199) and 824 (± 202) μm^2 for *Symbiodinium* sp. (Avir) and *E. voratum*, respectively, with no differences between the two species (*t*-test: $F_{5,5} = 1.033$, $P = 0.7799$). The average values for mitochondrial section area per cell were 258 (± 77) and 276 (± 51) μm^2 for *Symbiodinium* sp. (Avir) and *E. voratum*, respectively, with no differences between the two species (*t*-test: $F_{5,5} = 2.293$, $P = 0.6546$).

Growth, photosynthetic and respiratory adjustments during long-term exposure to an elevated temperature

We then exposed the two *Symbiodinium* sp. (Avir and Stylodid) to 32°C temperature conditions for 1 yr. Both strains were shown to be able to tolerate such temperatures over the course of a couple of wk (Dang *et al.*, 2019) but exhibited different degrees of photosynthesis to respiration coupling under an optimal range of temperatures (Figs 2, 3); that is, photosynthetic activity is not coupled to respiration in Avir and is coupled in Stylodid. The two *Symbiodinium* sp. displayed differential responses to long-

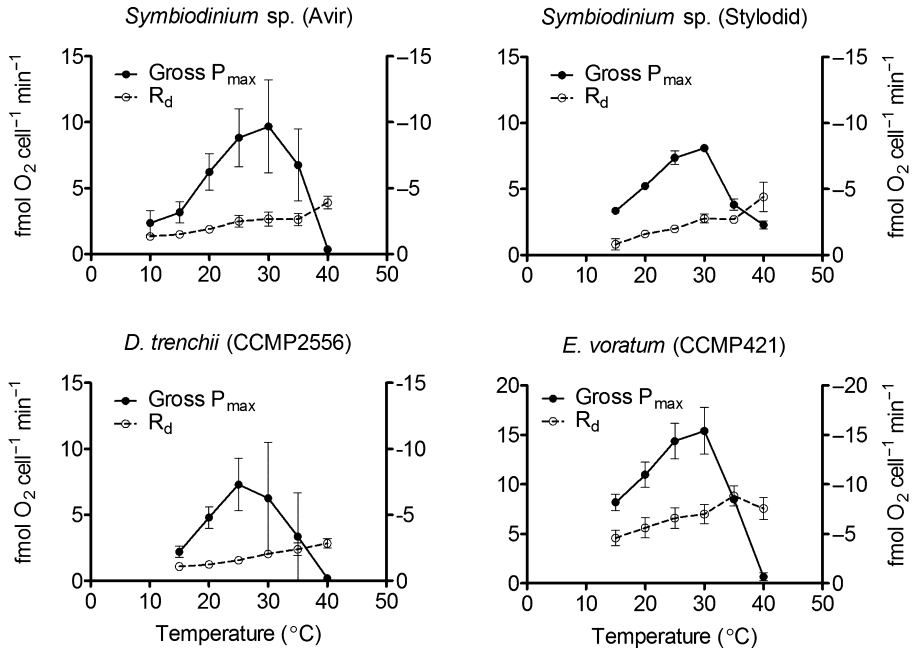

Fig. 1 Thermal response curves of gross maximal photosynthesis (P_{max}, left *y*-axis) and respiration (R_d, right *y*-axis) for *Symbiodinium* sp. (Avir), *Symbiodinium* sp. (Stylodid), *Durusdinium trenchii* and *Effrenium voratum* grown at 25°C. Measurements were performed for at least three independent culture replicates. The connecting line fits through the raw data. Vertical bars indicate the standard deviation.

Table 2 Cell-specific division rate (μ_c), photosynthetic characteristics (P vs I curves), dark respiration (R_d), and Chl cell contents of *Symbiodinium* sp. (Avir and Stylodid), *Durusdinium trenchii* (CCMP2556) and *Effrenium voratum* (CCMP421) cultivated at 25°C.

Species	μ_c (d^{-1})	Net P_{max} (fmol O_2 $cell^{-1}$ min^{-1})	Gross P_{max} (fmol O_2 $cell^{-1}$ min^{-1})	R_d (fmol O_2 $cell^{-1}$ min^{-1})	R_d : Gross P_{max}	Chl*a* (pg $cell^{-1}$)	Chl*c* (pg $cell^{-1}$)
Symbiodinium sp. (Avir)	0.41 (0.01)	5.4 (0.5)	7.5 (0.5)	–2.1 (0.3)	0.28 (0.03)	1.88 (0.21)	0.36 (0.08)
Symbiodinium sp. (Stylodid)	0.45 (0.04)	4.3 (0.3)	6.3 (0.6)	–2.0 (0.4)	0.32 (0.05)	1.54 (0.23)	0.60 (0.02)
D. trenchii	-	9.4 (1.0)	11.1 (1.3)	–1.6 (0.3)	0.15 (0.02)	0.99 (0.11)	0.34 (0.02)
E. voratum	0.58 (0.02)	9.1 (2.3)	17.5 (2.3)	–8.4 (2.2)	0.48 (0.11)	1.51 (0.44)	0.49 (0.14)

Values in brackets represent standard deviation ($n \geq 3$).

term exposure to elevated temperature. We measured a stable *c.* 37% increase in μ_c in *Symbiodinium* sp. (Avir) throughout 1-yr of warming (RM ANOVA: $F_{3,2,6} = 11.10$, $P = 0.0073$) (Fig. 5). For *Symbiodinium* sp. (Stylodid), μ_c was lower when cells were cultivated at 32°C, although it showed a mild recovery after 1 yr at this temperature (RM ANOVA: $F_{3,2,6} = 9.910$, $P = 0.0097$). With respect to photosynthesis, we measured a higher and stable maximal gross P after 7 months of cultivation at 32°C (RM ANOVA: $F_{2,5,10} = 5.819$, $P = 0.0211$) for *Symbiodinium* sp. (Avir) but no change of maximal gross P in *Symbiodinium* sp. (Stylodid) (RM ANOVA: $F_{2,5,10} = 2.857$, $P = 0.1043$) (Fig. 5). TRCs (Fig. 6) showed that both respiration rates and the slopes of respiratory TRCs declined (flattening of the slope and decline of E_a R) for *Symbiodinium* sp. (Avir) during the 1 yr of incubation at 32°C (Fig. 6b). This reflects a progressive decline in the temperature dependence of this metabolic process. By contrast, for *Symbiodinium* sp. (Stylodid), no change in respiration rates was observed (Fig. 6e). However, the comparison of E_a P with E_a R in *Symbiodinium* sp. (Stylodid) (Fig. 6f), indicates that exposure to 32°C conditions caused a divergence in the temperature dependence of photosynthesis and respiration (i.e. 2.2-fold higher E_a P than E_a R; *t*-test: $F_{5,5} = 9.756$, $P < 0.0001$), with respect to the cells growing at 25°C. This metabolic uncoupling is also reflected by the slight increase in net O_2 evolution (although not statistically significant after 1 yr; *t*-test: $F_{5,5} = 1.282$, $P = 0.0707$) in the presence of SHAM (Fig. S3), which is similar to the uncoupled phenotype of *Symbiodinium* sp. (Avir) (Fig. 3). However, for both *Symbiodinium* sp. (Avir) and (Stylodid), these photosynthetic and respiratory changes observed during the 1 yr of warming were rapidly reversed (within 1 wk) when cells were returned to the control conditions of 25°C (Figs S4, S5). For *Symbiodinium* sp. (Avir), the Chl*a* cell content declined from 1.9 to 1.4 pg $cell^{-1}$ during the 1-yr period at 32°C but recovered to 1.6 pg $cell^{-1}$ when cells were returned to 25°C (RM ANOVA: $F_{3,2,6} = 6.949$, $P = 0.0223$). For *Symbiodinium* sp. (Stylodid), no changes in the Chl*a* cell content were measured during the 1-yr period at 32°C (RM ANOVA: $F_{2,2,4} = 1.474$, $P = 0.3315$).

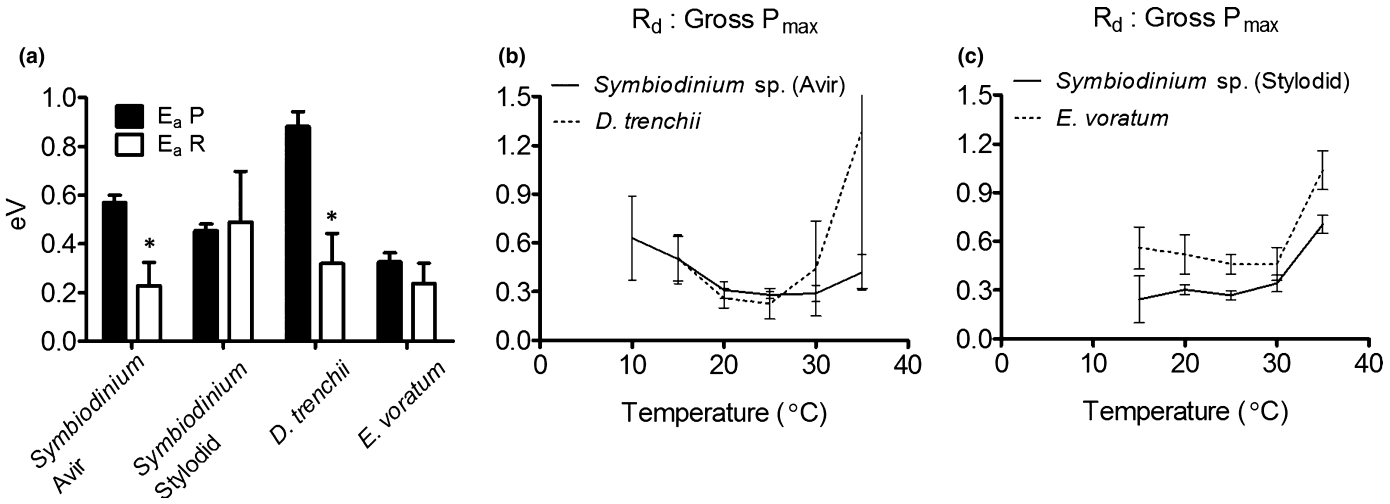

Fig. 2 (a) Comparison between activation energies (in electron volts, eV) of gross photosynthesis (E_a P) and respiration (E_a R) of *Symbiodinium* sp. (Avir), *Symbiodinium* sp. (Stylodid), *Durusdinium trenchii* and *Effrenium voratum* cultivated at 25°C. The E_a were extrapolated from the slopes of thermal response curves (Fig. 1) using the Arrhenius equation. Asterisks indicate statistically significant differences of E_a R in comparison to E_a P (*, $P < 0.05$). (b) Respiration (R_d) to gross maximal photosynthesis (P_{max}) ratios as a function of increasing temperature in *Symbiodinium* sp. (Avir) and *D. trenchii*. (c) R_d to gross P_{max} ratios as a function of increasing temperature in *Symbiodinium* sp. (Stylodid) and *E. voratum*. All measurements were performed for at least three independent culture replicates. The connecting line fits through the raw data. Vertical bars indicate the standard deviation.

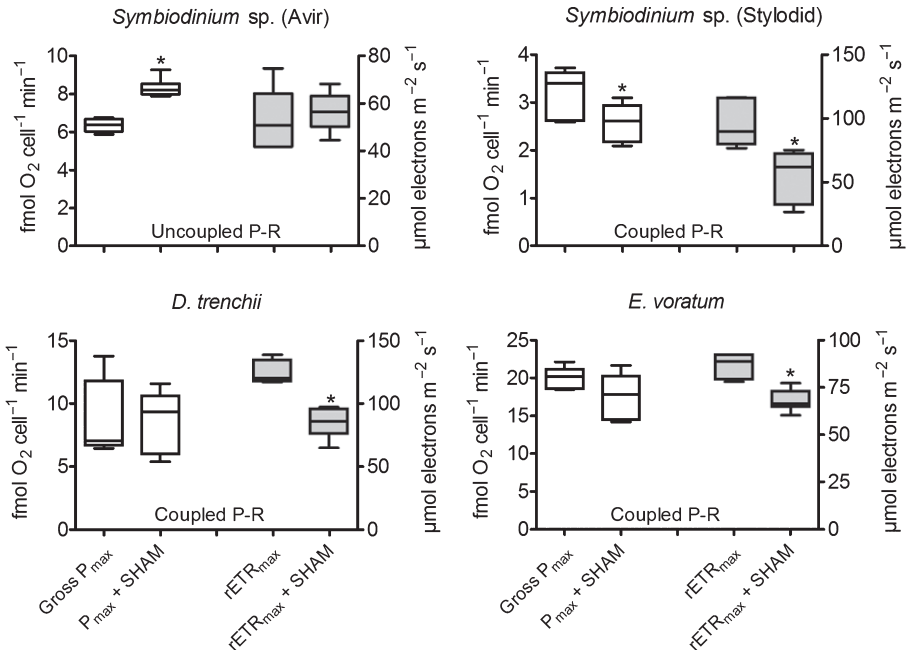

Fig. 3 Comparison of maximal gross oxygen evolution (gross P_{max}) and maximal relative electron transport rate of photosystem II ($rETR_{max}$) in *Symbiodinium* sp. (Avir), *Symbiodinium* sp. (Stylodid), *Durusdinium trenchii* and *Effrenium voratum*. Measurements were performed both in the absence and presence of salicylhydroxamic acid (SHAM), an inhibitor of mitochondrial alternative oxidase activity. All the measurements were performed for at least three independent culture replicates. Box plots show the interquartile range (box), median (horizontal line), and range (vertical bars). *, $P < 0.05$.

Photosynthetic affinity for CO_2 is enhanced during long-term exposure to an elevated temperature

The photosynthesis of *Symbiodinium* sp. (Avir) under different inorganic carbon availabilities was finally analysed (Fig. 7, Table 3). The slope of the CO_2-limited part of the curve was higher for cells grown at 32°C after 7 months and 1 yr ($n = 2$), than for cells cultivated at 25°C (one-way ANOVA: $F_{2,6} = 8.189$, $P = 0.0193$). The corresponding $K_{0.5}$ was not different between cells at 25 and 32°C (one-way ANOVA: $F_{2,6} = 1.462$, $P = 0.3040$). Neither the slope nor the the $K_{0.5}$ of the C_i-limited part of the curve measured for cells exposed to

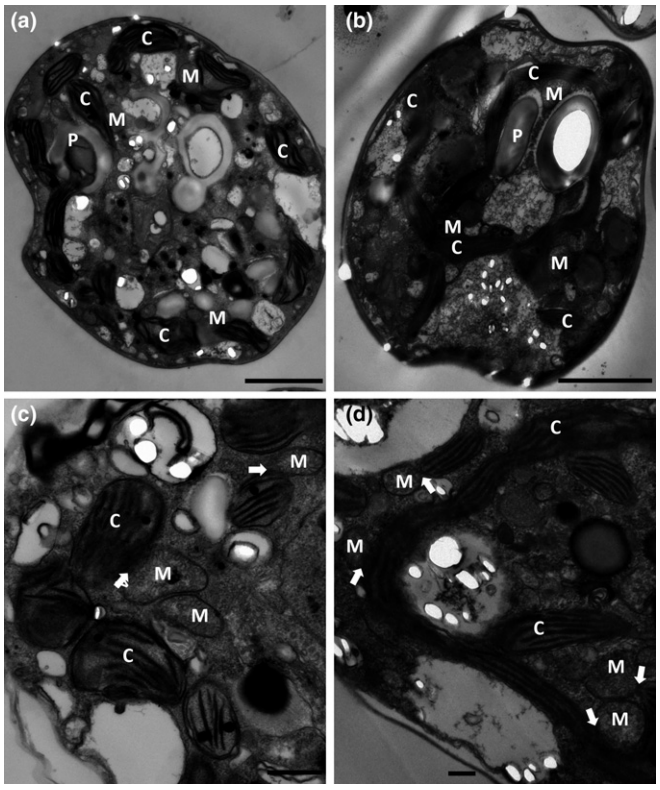

Fig. 4 Transmission electron micrographs illustrating subcellular organization of *Symbiodinium* sp. (Avir) (a, c) and *Effrenium voratum* (b, d). Arrows show the mitochondrial–chloroplastic contacts. Bars: 2 μm (a, b); 0.5 μm (c, d). C, chloroplast; M, mitochondria with tubular cristae; P, pyrenoid.

32°C conditions over the course of 1 yr were statistically different from the 25°C control condition (one-way ANOVA: $F_{2,6} = 3.727$, $P = 0.0887$; $F_{2,6} = 2.276$, $P = 0.1839$).

Discussion

In this study we have shown the following: first, Symbiodiniaceae species have different degrees of photosynthesis to respiration coupling; second, coupling between photosynthesis and respiration is strongly controlled by temperature, influencing how species respond to temperature changes; and third, photosynthesis to respiration coupling does not define the capability of species to adapt to long-term temperature increase.

Symbiodiniaceae have different metabolic thermal sensitivities

Thermal response curves for photosynthesis and respiration have been used to describe species' ability to cope with fluctuating temperature conditions (Karsten *et al.*, 2016; Prelle *et al.*, 2019) and adaptation to habitats with contrasting thermal regimes (Berry & Bjorkman, 1980; Collier *et al.*, 2017). Our TRCs showed that *Symbiodinium* sp. (Avir) can tolerate a wide range (10–35°C) of temperatures and rapidly fluctuating temperatures, in comparison to other Symbiodiniaceae. This could relate to the species' association to a host – a sea anemone, *Anemonia viridis*, which inhabits intertidal and sublittoral zones of temperate latitudes (Suggett *et al.*, 2012; Roberty *et al.*, 2016) (i.e. areas characterized by relatively wide daily and seasonal changes of temperature conditions, Table 1). By contrast, species as *D. trenchii*, which are found in tropical regions exposed to high thermal regimes (Pettay *et al.*, 2015; Silverstein *et al.*, 2015), exhibited the lowest tolerance to low (15°C) and/or oscillating temperatures.

Diverse degrees of photosynthesis and respiration thermal sensitivity reveal the coupling or uncoupling between the two energetic metabolisms

With regards to the TRCs, the comparisons between the temperature-dependent increases, in the 10–30°C range, of photosynthesis and respiration are of particular interest. In *Symbiodinium* sp. (Avir) and *D. trenchii*, respiration is less sensitive (lower E_a R, and declining R_d : gross P) than photosynthesis, and so metabolic changes appear uncoupled (Figs 1, 2). This is also consistent with the early work of Iglesias-Prieto *et al.* (1992) in which a lower temperature dependence of respiration in comparison to photosynthesis in *S. microadriaticum* was reported. By contrast, for *Symbiodinium* sp. (Stylodid) and *E. voratum*, we interpret the same temperature dependency of both respiration and

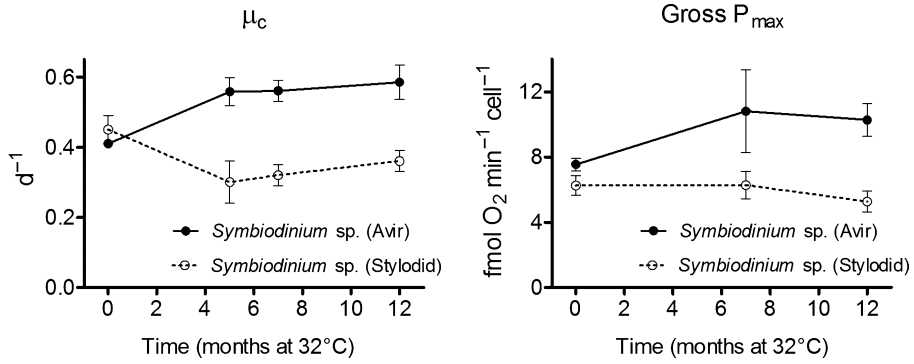

Fig. 5 Cell-specific division rate (μ_c) and gross maximal photosynthesis (Pmax) of *Symbiodinium* sp. (Avir) and *Symbiodinium* sp. (Stylodid) growing at 25°C (0 months) and during the 1-yr-long experiment at 32°C. Measurements were performed for at least three independent biological replicates. The connecting line fits through the raw data. Vertical bars indicate the standard deviation.

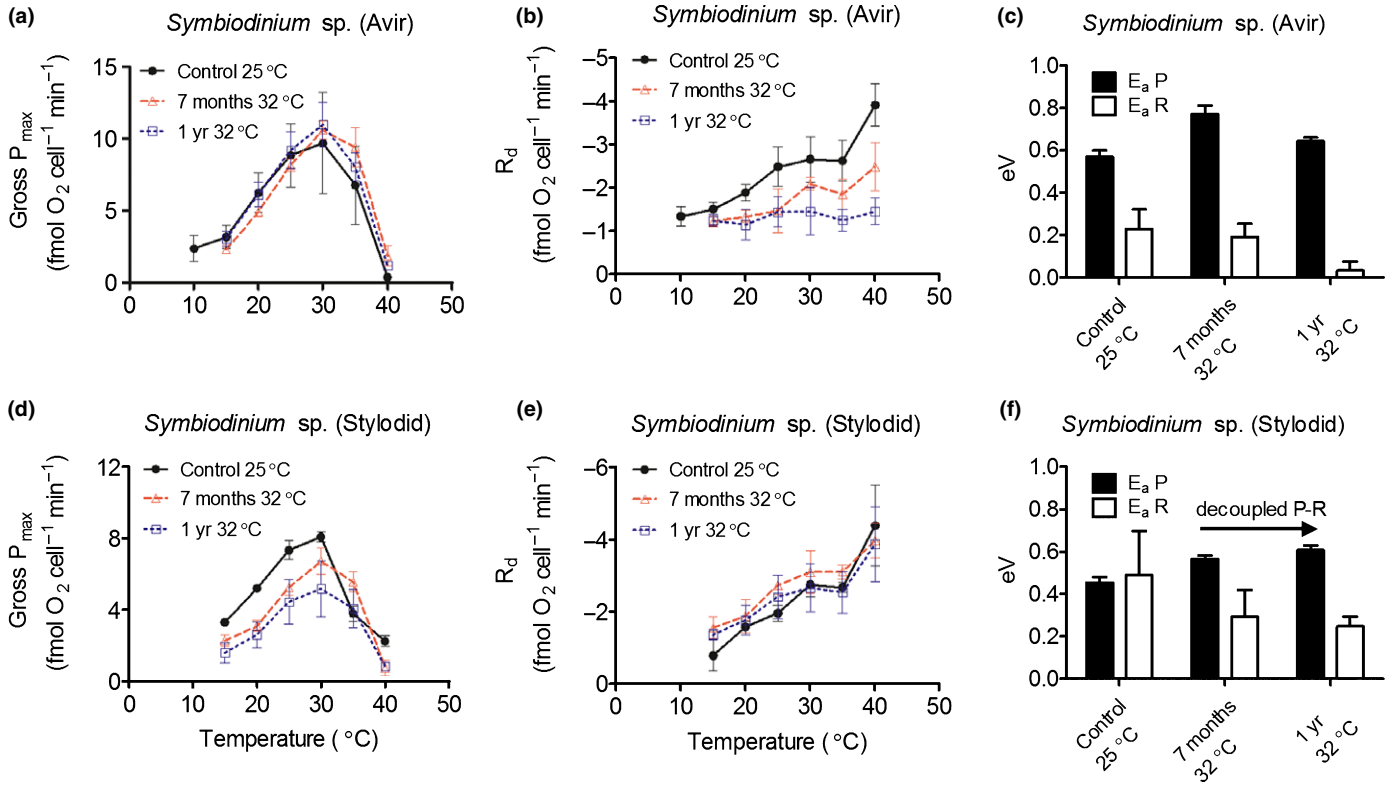

Fig. 6 Changes in thermal response curve characteristics during the 1-yr-long experiment at 32°C, in comparison to cells kept at 25°C. (a, d) Gross maximal photosynthesis (P_{max}) of *Symbiodinium* sp. (Avir) and *Symbiodinium* sp. (Stylodid). (b, e) Respiration (R_d) of *Symbiodinium* sp. (Avir) and *Symbiodinium* sp. (Stylodid). (c, f) Activation energies of gross photosynthesis (E_a P) and respiration (E_a R) of *Symbiodinium* sp. (Avir) and *Symbiodinium* sp. (Stylodid). All measurements were performed for at least three independent culture replicates. The connecting line fits through the raw data. Vertical bars indicate the standard deviation.

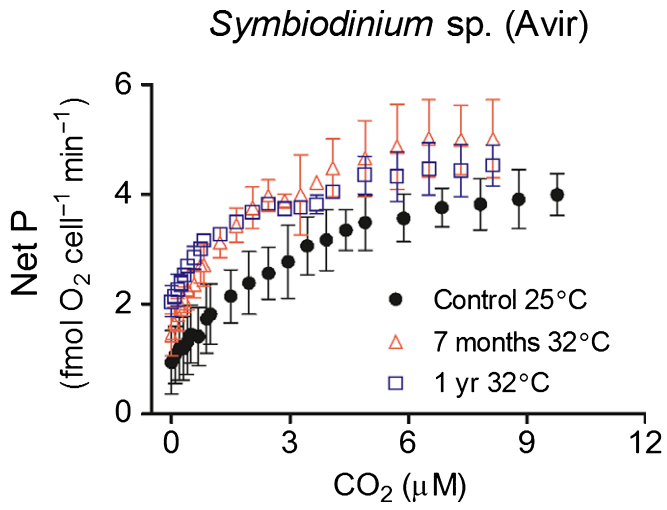

Fig. 7 Photosynthetic response to inorganic carbon (P vs CO_2 curves) of *Symbiodinium* sp. (Avir) when exposed to 25°C temperature conditions and during the 1-yr-long experiment at 32°C. Vertical bars indicate standard deviation of at least two independent replicates.

photosynthesis (same E_a for R and P, and constant R_d : gross P) as evidence that the two energetic processes are strongly coupled (Figs 1, 2). Analogue variations of respiration and photosynthesis in TRCs have been previously observed for green algae (Pierangelini *et al.*, 2019) and in a marine diatom (Schaum *et al.*, 2018), and they can be directly linked to the tight coupling of respiratory and photosynthetic activity in these organisms (e.g. the exchange of metabolic substrates and/or re-routing of the reducing power generated in the chloroplast towards mitochondria and the import of mitochondrial ATP into the chloroplast) (Cardol *et al.*, 2009; Bailleul *et al.*, 2015). Above 30°C, there is a rapid decline in photosynthesis but no negative effects on respiration, reflecting the lower sensitivity of this metabolic pathway to high temperatures (Iglesias-Prieto *et al.*, 1992; Grégoire *et al.*, 2017; Barton *et al.*, 2020), and showing that such temperatures disrupt the respiration–photosynthesis coupling. Taken together, the presence of an interspecific diversity in thermal metabolic sensitivity of Symbiodiniaceae reflects a differential degree of coupling between their photosynthetic and respiratory metabolisms.

Inhibition of respiration reveals the connection with photosynthesis

To further determine whether respiratory metabolism is coupled to photosynthesis, we compared the changes in photosynthetic O_2 evolution and rETR capacity caused by exposure to SHAM (Fig. 3). We reasoned that if photosynthesis depends on respiration, then an inhibition of respiration should affect

Table 3 Parameters extrapolated from the photosynthetic response to CO_2 and inorganic carbon (C_i) of *Symbiodinium* sp. (Avir) exposed to temperature conditions of 25°C and 1 yr at 32°C.

	Slope CO_2 (fmol O_2·cell^{-1} min^{-1} (μM CO_2)$^{-1}$)	$K_{0.5}$ CO_2 (μM)	Slope C_i (fmol O_2·cell^{-1} min^{-1} (μM^{-1} C_i)$^{-1}$)	$K_{0.5}$ C_i (μM)
25°C	0.78 (0.14)	11 (8)	0.0039 (0.0007)	307 (213)
32°C, 7 months	1.35 (0.25)*	5 (1)	0.0056 (0.0010)	134 (30)
32°C, 1 yr	1.35 (0.29)*	3 (1)	0.0056 (0.0012)	47 (25)

'Slope CO_2' is the slope of the CO_2-limited part of the P vs CO_2 curve (Fig. 7) (Ruan *et al*., 2017); $K_{0.5}$ CO_2 is the CO_2 concentration needed to give half-maximum photosynthetic activity; 'Slope C'$_i$ is the slope of the C_i-limited part of the P vs C_i curve (not shown); $K_{0.5}$ C_i is the C_i concentration needed to give half-maximum photosynthetic activity. Values in brackets represent standard deviation ($n \geq 2$). Asterisks indicate statistically significant differences from the 25°C condition (*, $P < 0.05$).

photosynthesis, as well. In *Symbiodinium* sp. (Stylodid) and *E. voratum*, inhibition of the AOX respiratory pathway was concomitant with a significant decrease in photosynthetic $rETR_{max}$. Since the inhibition of respiration has a greater impact on rETR than on maximal gross P, this suggests that an electron flow from water (i.e. at the PSII donor side) to oxygen (i.e. reduced by mitochondrial AOX) takes place in the absence of an inhibitor (Cardol *et al*., 2008; Roberty *et al*., 2014) in these species. This result is also very similar to that obtained for the marine diatom *Phaeodactylum tricornutum*, for which an interaction between the two metabolic processes is necessary to balance the levels of ATP and NADPH in the plastid (Bailleul *et al*., 2015; Murik *et al*., 2019). In the case of *Symbiodinium* sp. (Avir), we found no effect related to the inhibition of AOX on $rETR_{max}$. As in Symbiodiniaceae, AOX activity accounts for *c.* 25–30% of the respiration (Oakley *et al*., 2014b); the 30% increase of *Symbiodinium* sp. (Avir) maximal gross P could be related to a reduced O_2 consumption, rather than any effect on photosynthesis. These results provide further evidence that the photosynthetic activity of *Symbiodinium* sp. (Avir) is uncoupled from respiration. By contrast, photosynthesis of *D. trenchii* was downregulated when AOX activity was inhibited, reflecting the occurrence of metabolic coupling. However, for this species, this is in contrast to the different temperature dependences of photosynthesis and respiration observed in the TRCs. Thus, we describe *D. trenchii* as a phenotype with a photosynthesis coupled to respiratory activity, but its photosynthesis was easily disengaged from respiration, following exposure to (stressful) conditions such as low temperatures (onset of the TRCs).

Subcellular organization does not reflect physiological functioning

It has been suggested that a physiological coupling between photosynthesis and respiration could be favoured by an intracellular placing of mitochondria in close proximity to chloroplasts (Prihoda *et al*., 2012). Nonetheless, here we found that this positioning of organelles occurred in both *Symbiodinium* sp. (Avir) and *E. voratum*, regardless of their differential levels of photosynthesis–respiration interaction. This suggests that the cross-talk between mitochondria and chloroplasts is not related to their spatial organization, but rather to different capacities to exchange metabolites.

Our ultrastructural analysis seems also to indicate that in both *Symbiodinium* sp. (Avir) and *E. voratum,* as well as in other Symbiodiniaceae (Leggat *et al*., 2002; Shoguchi *et al*., 2013; Lee *et al*., 2015), some pyrenoids are not immersed in the chloroplast, as in green algae (Treves *et al*., 2016; Mackinder *et al*., 2017; Pierangelini *et al*., 2017) and haptophytes (Stojkovic *et al*., 2013; Heureux *et al*., 2017). This may suggest that this microcompartment may not necessarily work as proposed for the latter, that is, being the aggregation site of Rubisco, and favouring CO_2 accumulation in proximity to this enzyme (Meyer & Griffiths, 2013; Freeman Rosenzweig *et al*., 2017). However, we do not exclude the possibility that the pyrenoid position and functioning may change under environmental conditions regulating CCM activity or when *in hospite* (Leggat *et al*., 2002).

Photosynthesis–respiration coupling will not determine the adaptive response of Symbiodiniaceae to global warming

For species as *Symbiodinium* sp. (Avir), which are characterized by uncoupled photosynthesis–respiration, exposure to prolonged elevated temperature conditions (32°C) is expected to make photosynthetic and respiratory metabolisms work even more independently, without compromising cell growth. In particular, throughout the 1-yr period at 32°C, the photosynthetic metabolism of this species responded following the 'hotter is better' model (Jin & Agustí, 2018), with increased performance under hotter conditions but exhibiting susceptibility to lower temperatures (10°C, Fig. S1c). The higher photosynthetic performance could also be linked to a slight enhancement of the CCM activity, reflecting a higher cell need for CO_2. We must also point out that changes in both μ_c and photosynthetic performance showed no progressive increasing/decreasing trend during the 1-yr period (Fig. 5). The decline of $K_{0.5}$ C_i (although not statistically significant) observed here is also comparable to what was reported by Oakley *et al*. (2014a) after exposing Symbiodiniaceae to elevated temperature for a few wk. This indicates that the overall cell response arose shortly (within days) after exposure at 32°C temperatures, and thus, the changes are related to acclimation rather than adaptation. This is also supported by the quick recovery of photosynthesis when cells returned to 25°C conditions (Fig. S4).

In contrast to the increase in photosynthesis, respiration rates of *Symbiodinium* sp. (Avir) became progressively lower and less temperature dependent during the long-term warming period. Following the TRC respiration responses (type I and II) described for plants exposed to warm conditions (Atkin & Tjoelker, 2003; Smith & Dukes, 2013), our results show that the type I response (indicated by the lower slope of TRCs) and type II response (reduction in the elevation of TRCs) co-occur in *Symbiodinium* sp. (Avir) when cells are grown at an elevated temperature. Our results also show that the two responses take place over a different time

scale, with the type I response occurring later than the type II response. However, neither type I nor type II responses were adaptive, and respiratory metabolism was rapidly reversed when cells were returned from 32 to 25°C conditions.

In contrast to *Symbiodinium* sp. (Avir), for which photosynthesis is not coupled to respiration, other Symbiodiniaceae such as *Symbiodinium* sp. (Stylodid), which do exhibit photosynthesis–respiration coupling, will be more negatively affected by prolonged exposure to elevated temperature. Our results suggest that when *Symbiodinium* sp. (Stylodid) was cultivated at 32°C, interaction between photosynthetic and respiratory metabolism is prevented (showing higher E_a P than E_a R, Fig. S3), and despite the 1-yr acclimation time, adaptive responses to re-establish the connection between metabolisms did not occur. This probably contributed to the observed decrease in μ_c. Negative effects on cell growth in *Symbiodinium* sp. (Stylodid) were also reported by Dang *et al.* (2019), after 2 wk of exposure to high temperature conditions (33°C), supporting the occurrence of the μ_c decline shortly after heat exposure, and lack of adaptive response in this species.

Photosynthesis–respiration coupling might determine the metabolic compatibility between Symbiodiniaceae and their hosts

The presence of either a coupled or uncoupled photosynthetic activity to respiration in Symbiodiniaceae, may also have implications for our understanding of their life in symbiosis. It is known that when *in hospite*, the Symbiodiniaceae cell division is strictly controlled and reduced by the animal hosts (Falkowski *et al.*, 1993; Xiang *et al.*, 2020). As cell division is directly linked to respiratory metabolism (which converts carbohydrates produced during photosynthesis into cellular metabolites used in the construction of cells; Falkowski *et al.*, 1985; Geider & Osborne, 1989), respiration rates must also be kept low when *in hospite* (Rädecker *et al.*, 2018; M. Pierangelini, unpublished). However, at the same time, photosynthesis must be maintained in order to guarantee the translocation of the fixed carbon to the host (Matthews *et al.*, 2017, 2018; Krueger *et al.*, 2020). Thus, we put forward the idea that having photosynthetic activity which can function independently from respiration could represent an advantage for Symbiodiniaceae in establishing successful endosymbiosis. Nonetheless, the coupling of photosynthesis to respiration could still be advantageous to hosts by facilitating the coordination of the overall metabolic activity of the photosymbionts; that is, by directly controlling respiration, hosts can rule on photosynthesis, as well. Overall, our observations suggest that photosynthesis–respiration interaction could play a role in determining the metabolic compatibility between Symbiodiniaceae and their hosts (Morris *et al.*, 2019).

Conclusions

This work shows that the coupling between chloroplastic and mitochondrial energetic metabolisms occurs to different extents amongst Symbiodiniaceae. Species of this family are characterized by having photosynthetic activity that is either coupled to or uncoupled from respiratory metabolism (including intermediate phenotypes). The coupling between metabolisms is also disrupted upon changes in thermal conditions, both below and above the optimum, influencing how species perform during stable or fluctuating temperatures. During long-term exposure to high and/or above-optimal thermal regimes, the two Symbiodiniaceae (with a photosynthetic activity coupled or uncoupled to respiration) displayed no evidence of adaptation, despite the high numbers of cell generations (310 and 190 for *Symbiodinium* sp. (Avir) and (Stylodid), respectively). In both species, adjustments of energetic metabolism occurred shortly after heat exposure and were fully reversible even after the 1-yr period of warming. This suggests that neither a coupled nor an uncoupled phenotype provides an advantage in terms of defining the capacity of a given species to adapt to global warming. However, we cannot exclude the possibility that other responses have been developed in long-term heat-stressed cells (Chakravarti *et al.*, 2020). Ecologically, this lack of adaptive capabilities in Symbiodiniaceae confirms the susceptibility of coral reefs to ocean warming. At this stage, more studies are also necessary to predict the impact that one or another of these energetic metabolic traits will have on the susceptibility of the Symbiodiniaceae-hosts' endosymbiotic relationships to ocean warming.

Acknowledgements

PC acknowledges financial support from the Belgian Fonds de la Recherche Scientifique FRS–FNRS (PDR T.0032, CDR J.0079) and European Research Council (H2020-EU BEAL project 682580). We thank Annika Guse, Heidelberg University, for providing us with *D. trenchii*. We thank Stephane Roberty and Felix Vega de Luna for their help maintaining the algal cultures, genotyping of the species, assistance with fluorescence analyses, and valuable suggestions. We thank Nataly Hidalgo for her comments, supportive discussions and statistical advice. Finally, we thank the reviewers for their constructive comments. PC is Senior Research Associate from Fonds de la Recherche Scientifique – FNRS.

Author contributions

MP and PC conceived the research, analysed the data, and wrote the manuscript; MP performed the physiological analyses; MT performed the TEM analysis; all authors reviewed the manuscript.

ORCID

Pierre Cardol https://orcid.org/0000-0001-9799-0546
Mattia Pierangelini https://orcid.org/0000-0002-6166-8472
Marc Thiry https://orcid.org/0000-0002-4944-584X

References

Achlatis M, Pernice M, Green K, Guagliardo P, Kilburn MR, Hoegh-Guldberg O, Dove S. 2018. Single-cell measurement of ammonium and bicarbonate

uptake within a photosymbiotic bioeroding sponge. *The ISME Journal* **12**: 1308–1318.

Aranguren-Gassis M, Kremer CT, Klausmeier CA, Litchman E. 2019. Nitrogen limitation inhibits marine diatom adaptation to high temperatures. *Ecology Letters* **22**: 1860–1869.

Atkin OK, Scheurwater I, Pons TL. 2006. High thermal acclimation potential of both photosynthesis and respiration in two lowland *Plantago* species in contrast to an alpine congeneric. *Global Change Biology* **12**: 500–515.

Atkin OK, Tjoelker MG. 2003. Thermal acclimation and the dynamic response of plant respiration to temperature. *Trends in Plant Science* **8**: 343–351.

Bailleul B, Berne N, Murik O, Petroutsos D, Prihoda J, Tanaka A, Villanova V, Bligny R, Flori S, Falconet D *et al.* 2015. Energetic coupling between plastids and mitochondria drives CO_2 assimilation in diatoms. *Nature* **524**: 366–369.

Barton S, Jenkins J, Buckling A, Schaum CE, Smirnoff N, Raven JA, Yvon-Durocher G. 2020. Evolutionary temperature compensation of carbon fixation in marine phytoplankton. *Ecology Letters* **23**: 722–733.

Beardall J, Giordano M. 2002. Ecological implications of microalgal and cyanobacterial CO_2 concentrating mechanisms, and their regulation. *Functional Plant Biology* **29**: 335–347.

Berry J, Bjorkman O. 1980. Photosynthetic response and adaptation to temperature in higher plants. *Annual Review of Plant Physiology* **31**: 491–543.

Brading P, Warner ME, Davey P, Smith DJ, Achterberg EP, Suggett DJ. 2011. Differential effects of ocean acidification on growth and photosynthesis among phylotypes of *Symbiodinium* (Dinophyceae). *Limnology and Oceanography* **56**: 927–938.

Brading P, Warner ME, Smith DJ, Suggett DJ. 2013. Contrasting modes of inorganic carbon acquisition amongst *Symbiodinium* (Dinophyceae) phylotypes. *New Phytologist* **200**: 432–442.

Cardol P, Alric J, Girard-Bascou J, Franck F, Wollman FA, Finazzi G. 2009. Impaired respiration discloses the physiological significance of state transitions in *Chlamydomonas*. *Proceedings of the National Academy of Sciences, USA* **106**: 15979–15984.

Cardol P, Bailleul B, Rappaport F, Derelle E, Béal D, Breyton C, Bailey S, Wollman FA, Grossman A, Moreau H *et al.* 2008. An original adaptation of photosynthesis in the marine green alga *Ostreococcus*. *Proceedings of the National Academy of Sciences, USA* **105**: 7881–7886.

Chakravarti LJ, Beltran VH, van Oppen MJ. 2017. Rapid thermal adaptation in photosymbionts of reef-building corals. *Global Change Biology* **23**: 4675–4688.

Chakravarti LJ, Buerger P, Levin RA, van Oppen MJ. 2020. Gene regulation underpinning increased thermal tolerance in a laboratory-evolved coral photosymbiont. *Molecular Ecology* **29**: 1684–1703.

Chakravarti LJ, van Oppen MJ. 2018. Experimental evolution in coral photosymbionts as a tool to increase thermal tolerance. *Frontiers in Marine Science* **5**: 227.

Collier CJ, Ow YX, Langlois L, Uthicke S, Johansson CL, O'Brien KR, Hrebien V, Adams MP. 2017. Optimum temperatures for net primary productivity of three tropical seagrass species. *Frontiers in Plant Science* **8**: 1446.

Collins S. 2011. Many possible worlds: expanding the ecological scenarios in experimental evolution. *Evolutionary Biology* **38**: 3–14.

Comeau S, Cornwall CE, DeCarlo TM, Doo SS, Carpenter RC, McCulloch MT. 2019. Resistance to ocean acidification in coral reef taxa is not gained by acclimatization. *Nature Climate Change* **9**: 477–483.

Dang KV, Pierangelini M, Roberty S, Cardol P. 2019. Alternative photosynthetic electron transfers and bleaching phenotypes upon acute heat stress in *Symbiodinium* and *Breviolum* spp. (Symbiodiniaceae) in culture. *Frontiers in Marine Science* **6**: 656.

Falkowski PG, Dubinsky Z, Muscatine L, McCloskey L. 1993. Population control in symbiotic corals. *BioScience* **43**: 606–611.

Falkowski PG, Dubinsky Z, Wyman K. 1985. Growth-irradiance relationships in phytoplankton. *Limnology and Oceanography* **30**: 311–321.

Fordyce AJ, Ainsworth TD, Heron SF, Leggat W. 2019. Marine heatwave hotspots in coral reef environments: physical drivers, ecophysiological outcomes and impact upon structural complexity. *Frontiers in Marine Science* **6**: 498.

Freeman Rosenzweig ESF, Xu B, Cuellar LK, Martinez-Sanchez A, Schaffer M, Strauss M, Cartwright HN, Ronceray P, Plitzko JM, Förster F *et al.* 2017. The eukaryotic CO_2-concentrating organelle is liquid-like and exhibits dynamic reorganization. *Cell* **171**: 148–162.

Geider RJ, Osborne BA. 1989. Respiration and microalgal growth: a review of the quantitative relationship between dark respiration and growth. *New Phytologist* **112**: 327–341.

Genty B, Briantais JM, Baker NR. 1989. The relationship between the quantum yield of photosynthetic electron transport and quenching of chlorophyll fluorescence. *Biochimica et Biophysica Acta (BBA)-General Subjects* **990**: 87–92.

Giordano M, Beardall J, Raven JA. 2005. CO_2 concentrating mechanisms in algae: mechanisms, environmental modulation, and evolution. *Annual Review of Plant Biology* **56**: 99–131.

González-Pech RA, Bhattacharya D, Ragan MA, Chan CX. 2019. Genome evolution of coral reef symbionts as intracellular residents. *Trends in Ecology & Evolution* **34**: 799–806.

Goyen S, Camp EF, Fujise L, Lloyd A, Nitschke MR, LaJeunensse T, Kahlk T, Ralph PJ, Suggett D. 2019. Mass coral bleaching of *P. versipora* in Sydney Harbour driven by the 2015–2016 heatwave. *Coral Reefs* **38**: 815–830.

Grégoire V, Schmacka F, Coffroth MA, Karsten U. 2017. Photophysiological and thermal tolerance of various genotypes of the coral endosymbiont *Symbiodinium* sp. (Dinophyceae). *Journal of Applied Phycology* **29**: 1893–1905.

Heureux AM, Young JN, Whitney SM, Eason-Hubbard MR, Lee RB, Sharwood RE, Rickaby RE. 2017. The role of Rubisco kinetics and pyrenoid morphology in shaping the CCM of haptophyte microalgae. *Journal of Experimental Botany* **68**: 3959–3969.

Huertas IE, Rouco M, Lopez-Rodas V, Costas E. 2011. Warming will affect phytoplankton differently: evidence through a mechanistic approach. *Proceedings of the Royal Society B: Biological Sciences* **278**: 3534–3543.

Hughes TP, Barnes ML, Bellwood DR, Cinner JE, Cumming GS, Jackson JBC, Kleypas J, van de Leemput IA, Lough JM, Morrison TH *et al.* 2017a. Coral reefs in the Anthropocene. *Nature* **546**: 82–90.

Hughes TP, Kerry JT, Álvarez-Noriega M, Álvarez-Romero JG, Anderson KD, Baird AH, Babcock C, Beger M, Bellwood DR, Berkelmans R *et al.* 2017b. Global warming and recurrent mass bleaching of corals. *Nature* **543**: 373–377.

Hughes TP, Kerry JT, Baird AH, Connolly SR, Dietzel A, Eakin CM, Heron SF, Hoey AS, Hoogenboom MO, Liu G *et al.* 2018. Global warming transforms coral reef assemblages. *Nature* **556**: 492–496.

Hume BC, Ziegler M, Poulain J, Pochon X, Romac S, Boissin E, de Vargas C, Planes S, Wincker P, Voolstra CR. 2018. An improved primer set and amplification protocol with increased specificity and sensitivity targeting the *Symbiodinium* ITS2 region. *PeerJ* **6**: e4816.

Iglesias-Prieto R, Matta JL, Robins WA, Trench RK. 1992. Photosynthetic response to elevated temperature in the symbiotic dinoflagellate *Symbiodinium microadriaticum* in culture. *Proceedings of the National Academy of Sciences, USA* **89**: 10302–10305.

IPCC. 2014. Pachauri RK, Meyer LA, eds. *Climate change 2014: synthesis report. Contribution of Working Groups I, II and III to the Fifth assessment report of the intergovernmental panel on climate change.* Geneva, Switzerland.

Jin P, Agustí S. 2018. Fast adaptation of tropical diatoms to increased warming with trade-offs. *Scientific Reports* **8**: 1–10.

Karsten U, Herburger K, Holzinger A. 2016. Living in biological soil crust communities of African deserts—physiological traits of green algal *Klebsormidium* species (Streptophyta) to cope with desiccation, light and temperature gradients. *Journal of Plant Physiology* **194**: 2–12.

Karsten U, Holzinger A. 2012. Light, temperature, and desiccation effects on photosynthetic activity, and drought-induced ultrastructural changes in the green alga *Klebsormidium dissectum* (Streptophyta) from a high alpine soil crust. *Microbial Ecology* **63**: 51–63.

Kranz SA, Young JN, Hopkinson BM, Goldman JA, Tortell PD, Morel FM. 2015. Low temperature reduces the energetic requirement for the CO_2 concentrating mechanism in diatoms. *New Phytologist* **205**: 192–201.

Krueger T, Horwitz N, Bodin J, Giovani ME, Escrig S, Fine M, Meibom A. 2020. Intracellular competition for nitrogen controls dinoflagellate population density in corals. *Proceedings of the Royal Society B: Biological Sciences* **287**: 20200049.

Lajeunesse TC, Fitt WK, Schmidt GW. 2010. The reticulated chloroplasts of zooxanthellae (*Symbiodinium*) and differences in chlorophyll localization among life cycle stages. *Coral Reefs* **29**: 627.

LaJeunesse TC, Parkinson JE, Gabrielson PW, Jeong HJ, Reimer JD, Voolstra CR, Santos SR. 2018. Systematic revision of Symbiodiniaceae highlights the antiquity and diversity of coral endosymbionts. *Current Biology* **28**: 2570–2580.

Larosa V, Meneghesso A, La Rocca N, Steinbeck J, Hippler M, Szabo I, Morosinotto T. 2018. Mitochondria affect photosynthetic electron transport and photosensitivity in a green alga. *Plant Physiology* **176**: 2305–2314.

Lee SY, Jeong HJ, Kang NS, Jang TY, Jang SH, Lajeunesse TC. 2015. *Symbiodinium tridacnidorum* sp. nov., a dinoflagellate common to Indo-Pacific giant clams, and a revised morphological description of *Symbiodinium microadriaticum* Freudenthal, emended Trench & Blank. *European Journal of Phycology* **50**: 155–172.

Leggat W, Badger MR, Yellowlees D. 1999. Evidence for an inorganic carbon-concentrating mechanism in the symbiotic dinoflagellate *Symbiodinium* sp. *Plant Physiology* **121**: 1247–1255.

Leggat W, Marendy EM, Baillie B, Whitney SM, Ludwig M, Badger MR, Yellowlees D. 2002. Dinoflagellate symbioses: strategies and adaptations for the acquisition and fixation of inorganic carbon. *Functional Plant Biology* **29**: 309–322.

Lewis E, Wallace DWR. 1998. *Program developed for CO_2 system calculations.* Oak Ridge, TN, USA: ORNL/CDIAC-105, Carbon Dioxide Information Analysis Center.

Mackinder LC, Chen C, Leib RD, Patena W, Blum SR, Rodman M, Ramundo S, Adams CM, Jonikas MC. 2017. A spatial interactome reveals the protein organization of the algal CO_2-concentrating mechanism. *Cell* **171**: 133–147.

Malerba ME, Palacios MM, Palacios Delgado YM, Beardall J, Marshall DJ. 2018. Cell size, photosynthesis and the package effect: an artificial selection approach. *New Phytologist* **219**: 449–461.

Matthews JL, Crowder CM, Oakley CA, Lutz A, Roessner U, Meyer E, Grossman AR, Weis VM, Davy SK. 2017. Optimal nutrient exchange and immune responses operate in partner specificity in the cnidarian-dinoflagellate symbiosis. *Proceedings of the National Academy of Sciences, USA* **114**: 13194–13199.

Matthews JL, Oakley CA, Lutz A, Hillyer KE, Roessner U, Grossman AR, Weis VM, Davy SK. 2018. Partner switching and metabolic flux in a model cnidarian–dinoflagellate symbiosis. *Proceedings of the Royal Society B: Biological Sciences* **285**: 20182336.

Meyer M, Griffiths H. 2013. Origins and diversity of eukaryotic CO_2-concentrating mechanisms: lessons for the future. *Journal of Experimental Botany* **64**: 769–786.

Morris LA, Voolstra CR, Quigley KM, Bourne DG Bay LK. 2019. Nutrient availability and metabolism affect the stability of coral–Symbiodiniaceae symbioses. *Trends in Microbiology* **27**: 678–689.

Murik O, Tirichine L, Prihoda J, Thomas Y, Araújo WL, Allen AE, Fernie AR, Bowler C. 2019. Downregulation of mitochondrial alternative oxidase affects chloroplast function, redox status and stress response in a marine diatom. *New Phytologist* **221**: 1303–1316.

Oakley CA, Hopkinson BM, Schmidt GW. 2014b. Mitochondrial terminal alternative oxidase and its enhancement by thermal stress in the coral symbiont *Symbiodinium*. *Coral Reefs* **33**: 543–552.

Oakley CA, Schmidt GW, Hopkinson BM. 2014a. Thermal responses of *Symbiodinium* photosynthetic carbon assimilation. *Coral Reefs* **33**: 501–512.

Padfield D, Yvon-Durocher G, Buckling A, Jennings S, Yvon-Durocher G. 2016. Rapid evolution of metabolic traits explains thermal adaptation in phytoplankton. *Ecology Letters* **19**: 133–142.

Pettay DT, Wham DC, Smith RT, Iglesias-Prieto R, LaJeunesse TC. 2015. Microbial invasion of the Caribbean by an Indo-Pacific coral zooxanthella. *Proceedings of the National Academy of Sciences, USA* **112**: 7513–7518.

Pierangelini M, Glaser K, Mikhailyuk T, Karsten U, Holzinger A. 2019. Light and dehydration but not temperature drive photosynthetic adaptations of basal streptophytes (*Hormidiella*, *Streptosarcina* and *Streptofilum*) living in terrestrial habitats. *Microbial Ecology* 77: 380–393.

Pierangelini M, Ryšánek D, Lang I, Adlassnig W, Holzinger A. 2017. Terrestrial adaptation of green algae *Klebsormidium* and *Zygnema* (Charophyta) involves diversity in photosynthetic traits but not in CO_2 acquisition. *Planta* **246**: 971–986.

Pierangelini M, Stojkovic S, Orr PT, Beardall J. 2014. Elevated CO_2 causes changes in the photosynthetic apparatus of a toxic cyanobacterium, *Cylindrospermopsis raciborskii*. *Journal of Plant Physiology* **171**: 1091–1098.

Prelle LR, Graiff A, Gründling-Pfaff S, Sommer V, Kuriyama K, Karsten U. 2019. Photosynthesis and respiration of Baltic Sea benthic diatoms to changing environmental conditions and growth responses of selected species as affected by an adjacent peatland (Hütelmoor). *Frontiers in Microbiology* **10**: 1500.

Prihoda J, Tanaka A, de Paula WB, Allen JF, Tirichine L, Bowler C. 2012. Chloroplast-mitochondria cross-talk in diatoms. *Journal of Experimental Botany* **63**: 1543–1557.

Quigg A, Kotabova E, Jarešová J, Kaňa R, Šetlík J, Šedivá B, Komárek O, Prášil O. 2012. Photosynthesis in *Chromera velia* represents a simple system with high efficiency. *PLoS ONE* 7: e47036.

Rädecker N, Raina JB, Pernice M, Perna G, Guagliardo P, Kilburn MR, Aranda M, Voolstra CR. 2018. Using Aiptasia as a model to study metabolic interactions in cnidarian-*Symbiodinium* symbioses. *Frontiers in Physiology* **9**: 214.

Raghavendra AS, Padmasree K. 2003. Beneficial interactions of mitochondrial metabolism with photosynthetic carbon assimilation. *Trends in Plant Science* **8**: 546–553.

Ralph PJ, Gademann R. 2005. Rapid light curves: a powerful tool to assess photosynthetic activity. *Aquatic Botany* **82**: 222–237.

Raven JA, Beardall J, Sánchez-Baracaldo P. 2017. The possible evolution and future of CO_2-concentrating mechanisms. *Journal of Experimental Botany* **68**: 3701–3716.

Ritchie RJ. 2006. Consistent sets of spectrophotometric chlorophyll equations for acetone, methanol and ethanol solvents. *Photosynthesis Research* **89**: 27–41.

Roberty S, Bailleul B, Berne N, Franck F, Cardol P. 2014. PSI Mehler reaction is the main alternative photosynthetic electron pathway in *Symbiodinium* sp., symbiotic dinoflagellates of cnidarians. *New Phytologist* **204**: 81–91.

Roberty S, Furla P, Plumier JC. 2016. Differential antioxidant response between two *Symbiodinium* species from contrasting environments. *Plant, Cell & Environment* **39**: 2713–2724.

Ros M, Camp EF, Hughes DJ, Crosswell JR, Warner ME, Leggat WP, Suggett DJ. 2020. Unlocking the black-box of inorganic carbon-uptake and utilization strategies among coral endosymbionts (Symbiodiniaceae). *Limnology and Oceanography*. doi: 10.1002/lno.11416.

Ruan Z, Raven JA, Giordano M. 2017. In *Synechococcus* sp. competition for energy between assimilation and acquisition of C and those of N only occurs when growth is light limited. *Journal of Experimental Botany* **68**: 3829–3839.

Schaum CE, Barton S, Bestion E, Buckling A, Garcia-Carreras B, Lopez P, Lowe L, Pawar S, Smirnoff N, Trimmer M *et al.* 2017. Adaptation of phytoplankton to a decade of experimental warming linked to increased photosynthesis. *Nature Ecology & Evolution* **1**: 1–7.

Schaum CE, Buckling A, Smirnoff N, Studholme DJ, Yvon-Durocher G. 2018. Environmental fluctuations accelerate molecular evolution of thermal tolerance in a marine diatom. *Nature Communications* **9**: 1–14.

Shoguchi E, Shinzato C, Kawashima T, Gyoja F, Mungpakdee S, Koyanagi R, Takeuchi T, Hisata K, Tanaka M, Fujiwara M *et al.* 2013. Draft assembly of the *Symbiodinium minutum* nuclear genome reveals dinoflagellate gene structure. *Current Biology* **23**: 1399–1408.

Silverstein RN, Cunning R, Baker AC. 2015. Change in algal symbiont communities after bleaching, not prior heat exposure, increases heat tolerance of reef corals. *Global Change Biology* **21**: 236–249.

Smith NG, Dukes JS. 2013. Plant respiration and photosynthesis in global-scale models: incorporating acclimation to temperature and CO_2. *Global Change Biology* **19**: 45–63.

Spalding MD, Brown BE. 2015. Warm-water coral reefs and climate change. *Science* **350**: 769–771.

Stojkovic S, Beardall J, Matear R. 2013. CO_2-concentrating mechanisms in three southern hemisphere strains of *Emiliania huxleyi*. *Journal of Phycology* **49**: 670–679.

Suggett DJ, Hall-Spencer JM, Rodolfo-Metalpa R, Boatman TG, Payton R, Pettay DT, Johnson VR, Warner ME, Lawson T. 2012. Sea anemones may thrive in a high CO_2 world. *Global Change Biology* **18**: 3015–3025.

Suggett DJ, Warner ME, Leggat W. 2017. Symbiotic dinoflagellate functional diversity mediates coral survival under ecological crisis. *Trends in Ecology & Evolution* **32**: 735–745.

Tcherkez GG, Farquhar GD, Andrews TJ. 2006. Despite slow catalysis and confused substrate specificity, all ribulose bisphosphate carboxylases may be nearly perfectly optimized. *Proceedings of the National Academy of Sciences, USA* **103**: 7246–7251.

Torda G, Donelson JM, Aranda M, Barshis DJ, Bay L, Berumen ML, Bourne DG, Cantin N, Foret S, Matz M *et al.* 2017. Rapid adaptive responses to climate change in corals. *Nature Climate Change* **7**: 627–636.

Treves H, Raanan H, Kedem I, Murik O, Keren N, Zer H, Berkowicz SM, Giordano M, Norici A, Shotland Y *et al.* 2016. The mechanisms whereby the green alga *Chlorella ohadii*, isolated from desert soil crust, exhibits unparalleled photodamage resistance. *New Phytologist* **210**: 1229–1243.

Vega de Luna F, Dang KV, Cardol M, Roberty S, Cardol P. 2019. Photosynthetic capacity of the endosymbiotic dinoflagellate *Cladocopium* sp. is preserved during digestion of its jellyfish host *Mastigias papua* by the anemone *Entacmaea medusivora*. *FEMS Microbiology Ecology* **95**: fiz141.

Weber MX, Medina M. 2012. The role of microalgal symbionts (*Symbiodinium*) in holobiont physiology. In: Piganeau G, ed. *Advances in botanical research, genomic insights into the biology of algae*. London, UK: Elsevier Associated Press, 119–140.

Xiang T, Lehnert E, Jinkerson RE, Clowez S, Kim RG, DeNofrio JC, Pringle JR, Grossman AR. 2020. Symbiont population control by host–symbiont metabolic interaction in Symbiodiniaceae–cnidarian associations. *Nature Communications* **11**: 1–9.

Supporting Information

Additional Supporting Information may be found online in the Supporting Information section at the end of the article.

Fig. S1 Comparison of thermal response curves started at 10 and 15°C, for gross maximal photosynthesis and respiration of *Symbiodinium* sp. (Avir) cultivated at 25 and 32°C.

Fig. S2 Transmission electron micrographs illustrating subcellular organization of *Symbiodinium* sp. (Avir) and *Effrenium voratum*.

Fig. S3 Comparison of maximal net oxygen evolution and maximal electron transport rate of photosystem II in *Symbiodinium* sp. (Stylodid) cultivated at 32°C for 7 months and 1 yr.

Fig. S4 P vs I curves of *Symbiodinium* sp. (Avir) and *Symbiodinium* sp. (Stylodid) showing the recovery of their gross photosynthetic activities when cells cultivated at 32°C were returned to 25°C conditions.

Fig. S5 Thermal response curves for *Symbiodinium* sp. (Avir) showing the recovery of the respiration activity and activation energy of respiration when cells cultivated 32°C were returned to 25°C conditions.

Please note: Wiley-Blackwell are not responsible for the content or functionality of any supporting information supplied by the authors. Any queries (other than missing material) should be directed to the *New Phytologist* Central Office.